



TRIBHUVAN UNIVERSITY
INSTITUTE OF ENGINEERING
PULCHOWK CAMPUS

**Integrated Control System for Active Fin-controlled Rocket Stabilization and
Guidance**

By:

Manish Tajpuriya (077BAS023)
Simonkrith Lamichhane (077BAS042)
Simran Paudel (077BAS043)
Sugam Lamsal (077BAS044)

A MID-TERM REPORT TO THE DEPARTMENT OF MECHANICAL AND
AEROSPACE ENGINEERING IN PARTIAL FULFILLMENT OF THE REQUIREMENT
FOR THE BACHELOR'S DEGREE IN AEROSPACE ENGINEERING

DEPARTMENT OF MECHANICAL AND AEROSPACE ENGINEERING
LALITPUR, NEPAL

December, 2024

ACKNOWLEDGEMENT

This project is prepared in partial fulfillment of the requirement for the bachelor's degree in Aerospace Engineering. First and foremost, we would like to express our sincere gratitude towards Dr.Sudip Bhattacharai, our project supervisor for his constant guidance, inspiring lectures and precious encouragement. Without his invaluable supervision and suggestions, it would have been a difficult journey for us. His useful suggestions for this whole work and cooperative behavior are sincerely acknowledged.

We would like to thank the Department of Mechanical and Aerospace Engineering, Institute of Engineering, Pulchowk Campus for providing us opportunity of collaborative undertaking which has helped us to implement the knowledge gained over these years as major project for fourth year, and develop a major project of our own that has greatly enhanced our knowledge and provided us a new experience of teamwork.

We would like to acknowledge Incubation, Innovation Entrepreneurship Center (IIEC), IOE Pulchowk Campus for providing us space and resources.

We would also like to thank all junior and senior members of SRB team who have constantly helped us in doing this project, without them the project would not have made this much progress.

Any kind of suggestion or criticism will be highly appreciated and acknowledged.

Authors:

Manish Tajpuriya
Simonkrith Lsmichhane
Simran Paudel
Sugam Lamsal

ABSTRACT

Active-fin control has become a special part of space launch vehicles and military applications. This contributes to improving the accuracy and reliability of modern rockets. The main objective of this project is to develop and demonstrate the active-fins control mechanism that enhances the rocket's stability and trajectory control. In this project, real-time sensor data such as IMU and GPS will be handled using sophisticated control algorithms to dynamically modify fin positions and guarantee desired flight routes. The project aims to enhance flight stability and trajectory accuracy. The project's main findings are expected to demonstrate improved stability and trajectory precision.

Keywords: Active-fins control, Control algorithm, Rockets, Stability, Trajectory

TABLE OF CONTENTS

TITLE PAGE	i
ACKNOWLEDGEMENT	ii
ABSTRACT	iii
TABLE OF CONTENTS	vi
LIST OF FIGURES	ix
LIST OF TABLES	x
LIST OF ABBREVIATIONS	xi
1 INTRODUCTION	1
1.1 Background	1
1.2 Problem Statement	1
1.3 Objectives	1
1.4 Application/Features	2
1.5 Feasibility Analysis	2
1.5.1 Economic Feasibility	2
1.5.2 Technical Feasibility	3
1.5.3 Operational Feasibility	3
1.6 System Requirements	4
1.6.1 Hardware Requirements	4
1.6.2 Software Requirements	4
1.6.3 Material Requirements	5
2 LITERATURE REVIEW	6
3 THEORETICAL BACKGROUND	8
3.1 Rocket Theory	8
3.1.1 Forces on Rocket	9
3.1.2 Stability	9
3.1.3 Propellant Theory	11
3.1.4 Nozzle Theory	13
3.2 Control System	14
3.3 PID	15

3.4	Kalman Filter	16
3.5	Computational Fluid Dynamics (CFD)	18
4	METHODOLOGY	19
4.1	Control system	19
4.1.1	Mathematical Modeling	20
4.1.2	Control system Algorithm	21
4.2	Flight Computer Development	22
4.2.1	Schematic Representation	22
4.2.2	Programming Algorithm	23
4.2.3	PCB Designing and Fabrication	23
4.3	Vehicle Development	25
4.3.1	Body Fabrication	25
4.3.2	Propulsion System	27
4.3.3	Nose Cone and Fins	30
4.3.4	Recovery System	30
4.3.5	Servo Housing and Linkages	31
4.4	Stability Analysis	31
4.4.1	Selection of fins	32
4.4.2	Static Stability Analysis	33
4.4.3	CFD Analysis	34
4.5	Wind Tunnel Testing	34
4.6	Servo Selection	35
5	RESULTS AND DISCUSSIONS	37
5.1	Output	37
5.1.1	Static Thrust Test	37
5.1.2	Wind Tunnel Test	37
5.1.3	Recovery Test	38
5.2	Work Completed	38
5.2.1	Propellant test	39
5.2.2	Nozzle Fabrication	41
5.2.3	Catapult Test	42
5.3	Work Remaining	42
5.4	Limitations	43
5.5	Problems Faced	43
5.6	Budget Analysis	43
5.7	Gantt chart	44

6 CONCLUSION AND FUTURE ENHANCEMENT	45
6.1 Conclusion	45
6.2 Scope For Future enhancement	45
REFERENCES	46

List of Figures

3.1 Flight Profile	8
3.2 Forces acting on Rocket in Free Flight	9
3.3 Location of CG and CP	10
3.4 Thrust Profile for different grain profiles	13
3.5 PID controller with feedback loop	15
4.1 Methodology	19
4.2 Control system	20
4.3 Control system Programming Algorithm	21
4.4 Flight Computer Schematic	22
4.5 Main Programming Algorithm	23
4.6 PCB Schematic and PCB Design	24
4.7 Avionics Bay	25
4.8 Design and Fabrication of Phase I	26
4.9 CAD Design of Phase II	26
4.10 Fabrication of Phase II	26
4.11 Propellant Grain of KNDX Propellant	27
4.12 Setup for Static Thrust Measurement	28
4.13 Composite Rocket Motor	29
4.14 Fabrication of Nozzle using Lathe	29
4.15 Graphite Nozzle	30

4.16	Motor For Black Powder Propellant	30
4.17	Fragments of Motor After Test	30
4.18	Servo Housing and Linkages	31
4.19	Stability Analysis	32
4.20	Airfoil Selection and Closeup	33
4.21	Shape Selection and Closeup	33
4.22	Rocket Design in OpenRocket	33
4.23	Baseline vs Optimized Fin	34
4.24	Properties of Optimized Fins	34
4.25	Wind Tunnel Flowchart	35
4.26	Setup for Wind Tunnel Test	35
4.27	Lag Response Test of SG90	36
5.1	Static Thrust Test I	37
5.2	Static Thrust Test II	37
5.3	Wind Tunnel Test	37
5.4	Wind Tunnel Test	38
5.5	Motor For Black Powder Propellant	40
5.6	Fragments of Motor After Test	40
5.7	Burnt Motor After Test	40
5.8	Mold for Composite Nozzle	41
5.9	Composite Nozzle	41
5.10	Bush Nozzle with Mseal as Convergent and Divergent Section	41

5.11 Sheet Metal Nozzle	41
5.12 Catapult Test	42
5.13 Timeline	44

List of Tables

1.1	Hardware Requirements	4
1.2	Software Requirements	4
1.3	Materials Requirements	5
4.1	Flight Computer 1 V/s Flight Computer 2	23
5.1	Formulation Table for KNSU Propellant	39
5.2	Formulation Table for Black Powder Propellant	39
5.3	Formulation Table for RNX-57 Propellant Mixture	40
5.4	Budget Analysis	43

LIST OF ABBREVIATIONS

CAAN	Civil Aviation Authority of Nepal
CD	Convergent-Divergent
CFD	Computational Fluid Dynamics
CG	Centre of Gravity
CP	Centre of Pressure
DoF	Degree Of Freedom
EKF	Extended Kalman Filter
FSI	Fluid Structure Interaction
GPS	Global Positioning System
HCL	Hydrochloric acid
IMU	Inertial Measurement unit
KF	Kalman Filter
KNSU	Potassium Nitrate Sucrose
KNDX	Potassium Nitrate Dextrose
LAR	Low Aspect Ratio
LQR	Linear Quadratic Regulator
MAR	Medium Aspect Ratio
MPC	Model Predictive Control
MOHA	Ministry of Home Affairs
O/F	Oxygen Fuel
PCB	Printed Circuit Board
PID	Proportional Integral Derivative
MAR	Moderate Aspect Ratio
ULAR	Ultra Low Aspect Ratio

1. INTRODUCTION

1.1. Background

The history of rocketry dates back to ancient times, with the earliest recorded use of rockets in China during the Song dynasty (960–1279 AD) for military purposes. These early rockets were simple, unguided, and often unstable in flight. During World War II, the German V-2 rocket became the first long-range guided ballistic missile, incorporating rudimentary stabilization and guidance systems using gyroscopes and movable fins. In the present time, active fin-controlled systems have varying applications which include modern military applications like guided missiles and artillery rockets for enhanced accuracy and effectiveness. Active fin-controlled rocket stabilization and guidance is an integrated control system used to improve the flight stability and accuracy of the rocket's trajectory by dynamically adjusting the orientation of fins based on real-time flight data. This makes it useful for launching and guiding rockets to a precise trajectory that enhances the mission success rate.

1.2. Problem Statement

A rocket without an active guidance system has limited applications in real-world scenarios due to its restricted maneuverability and stringent launch conditions. However, with the integration of active control systems in the rocket like stability and trajectory control in our case, its potential expands significantly. The success of a rocket's mission is heavily dependent on the trajectory it follows providing a narrow error margin. As rocket missions require extensive funding and precision, even a small error means a huge loss in mission objectives and finances. In extreme cases, even human life could be in danger due to inaccuracies. Hence, it is extremely crucial to have active stability, guidance, or both in a rocket system.

1.3. Objectives

Main Objective

- To actively control the rocket as desired during its flight using active fins.

Specific Objectives

- To develop a control system for the stability and guidance of a rocket.
- To ensure optimum control authority of control surfaces for rectifying lag responses.
- To optimize the fin configuration for optimum aerodynamic performance.

1.4. Application/Features

- Guidance: The active control system can be used to guide a rocket to follow a certain trajectory.
- Satellite deployment: Guided rockets are essential for placing satellites into precise orbits around Earth, ensuring they achieve the correct altitude and orientation for their missions.
- Research: Guided suborbital rockets are used for experiments that require brief exposure to space conditions or microgravity, such as biological studies or physics experiments.
- Defense system: The active fins can be used in making missiles for defense purposes.
- Recovery: In multi-stage rockets, the first part to separate is usually the booster which can be recovered with an additional contribution of active control fins.

1.5. Feasibility Analysis

1.5.1. Economic Feasibility

Integrating active guidance systems into rockets requires a substantial initial investment, but the benefits outweigh the costs. Reduced mission failure rates, the potential for re-usability, and available funding from government and private sectors provide strong financial incentives. Expenses can also be managed by making efficient material choices, streamlining design processes, and utilizing available resources. While upfront costs are high, long-term savings and increased mission success rates make this investment economically viable.

1.5.2. Technical Feasibility

The technical foundation for developing an active fins rocket is well-established. Key technologies, such as control mechanisms using servo motors and sensors like gyroscopes and accelerometers, are readily available. Consistent power supply is achievable with power management systems. Reliable real-time telemetry communication systems and simulation tools for performance optimization are also accessible. This demonstrates the strong technical feasibility of this project besides the wind tunnel which is only suitable for validation in low-velocity regions.

1.5.3. Operational Feasibility

CAAN is responsible for the safe and efficient execution of rocket activities in Nepal. It is essential to obtain regulations and permissions from CAAN for rocket operations, including a Rocket Launch Permit, which specifies launch details and ensures safety compliance. CAAN performs a comprehensive safety assessment, evaluating the launch trajectory and possible impacts on surrounding areas to identify and mitigate risks, prioritizing the safety of airspace users and the public.

MOHA's responsibilities in Nepal include public safety, security, and emergency management. Depending on the project, specific regulations and MOHA permissions may be required, such as security clearances for project personnel to ensure reliability and protect sensitive information. Coordination with law enforcement may be necessary to address security issues and establish appropriate measures. Compliance with MOHA's safety regulations, including protocols for handling hazardous materials and emergency response plans, is essential to maintain a safe operational environment and demonstrate a commitment to public safety and security.

1.6. System Requirements

1.6.1. Hardware Requirements

Hardware	Applications
Teensy 4.1, ESP32, Arduino	Micro-controllers
BNO 085, MPU6050, MPU9250	IMU sensing
Servo Motors(BMS-127WV+, Sg90)	Actuation of Fins
Load Cell	Thrust measurement
HX711	Amplifier
Li-ion/Li-Po Batteries	Power Supply
SD Card Module, SD card, Flash Chip	Data storage
LED, Buzzers	Indication system
BMP180, BMP280	Altitude Sensing
GPS Module	Navigation
LoRa Module	Communication
3D printer	Components Fabrication
Laser cutter	Cutting
Lathe Machine, CNC Machining	Nozzle Machining

Table 1.1: Hardware Requirements

1.6.2. Software Requirements

Software	Applications
MATLAB	Calculation, graphs
Simulink	Control System Design, Simulation and Analysis
Arduino IDE and VS code	Programming
CATIA V5, SOLIDWORKS and Fusion 360	CAD Design
Open Rocket	Rocket Design and Simulation
Ansys	Aerodynamics Simulation
RDWorks	CNC Laser Cutter
UPstudio , Bambu Studio	3D Printing

Table 1.2: Software Requirements

1.6.3. Material Requirements

Materials	Applications
Conc. HCL, Hydrogen Peroxide	PCB Fabrication
KNO_3 , Sucrose, Dextrose	Propellant
Epoxy, Hardener, Glass fiber, Carbon fiber	Composite Body Fabrication
Silicone Grease	Flame Protection
Mild Steel, Graphite, Cement	Nozzle Fabrication

Table 1.3: Materials Requirements

2. LITERATURE REVIEW

The active control of the rocket can be achieved with the application of control surfaces and thrust vectoring. The usual control surfaces of a rocket are canard and fins. Any of them can be made mobile to actively guide a rocket. The major problem with canard control design is roll reversal. The vortical flows arising from the canard changes the pressure distribution on stabilizer surface and can cause a large rolling moment in the reverse direction. When the roll reversal phenomenon occurs the vehicle rotates in the reverse direction of the roll command. In this situation, the control system will be improper unless this phenomenon can be predicted and accounted for in advance which requires extensive simulation. The amount of this induced rolling moment on stabilizers depends on some parameters such as: aerodynamics geometry, control surface deflection angle, vehicle angle of attack and flight velocity [1].

There are standard fin configurations as trapezoidal, elliptical, clipped delta, rectangular and grid. Theoretically, elliptical fins are ideal as they provide the best lifting force; however, they also produce enough induced drag to also provide drag stability to the rocket. Clipped Delta fins are primarily used on high performance rockets to yield a low drag force. The elliptical and clipped delta configurations provided more positive figures of merit compared to the other types of fins [2]. But there are many rockets that don't follow the fixed geometrical shape because of some limitations and through computational analysis they created their own configuration as Samurai Sounder [3] and Shark caved [2]. Based on the aspect ratio of the fins, three types of fins are defined; MAR, LAR and ULAR. The behaviour of MAR and LAR is similar since both types of fins generate lift mainly through circulation. On the other hand, ULAR fins generate lift due to the pressure distribution created by the wing tip or leading edge vortices, for rectangular or delta platforms respectively.[4]

The fundamental problem in model rockets is the cost of in-plant tuning, since each iteration, or flight, needs of a new motor, in addition to the risk of destroying the model in the process[4]. Until now, PID controllers are the most popular controller used in rocket control systems due to their simplicity and satisfactory performances. This is because the implementation of PID controller is fairly easy to understand, build and tune. But a common problem occurred in PID control is noise produced by any real sensor[5].

The inevitable part of any control problem is modeling the process or plant. With the advent of fast processors and numerical software like MATLAB®, Maple®, Python®, etc., it is now possible to take a complex non-linear 6-DoF equation like that of a rocket and run a program that can trim and linearize it with ease[6]. The aerodynamics of the rocket body

are computed with the Extended Modified Barrowman Equations developed by Barrowman, Galejs and modified by the author. The actuator dynamics also have a detrimental effect in the stability of the rocket, in consequence, the actuator must also be modeled.[4]

The data received through sensors often contains significant noise, necessitating real-time filtering. This is achieved through various algorithms. The ultimate goal of algorithms research is to find an optimal solution for a given problem. Although it is rare to find a completely optimal algorithm for most problem domains, one exception is Bayesian state estimation. Here, the Kalman Filter, an algorithm that propagates a system's varying quantities over time, can be shown to be the best algorithm possible for its domain. At its core, it propagates a state characterized by a Gaussian distribution using linear transition functions in an optimal way. Since it is optimal, it has remained relatively unchanged since it was first introduced, but has received many extensions to apply it to more than just linear Gaussian systems. The EKF exemplifies this by linearizing nonlinear transition and observation functions using a Taylor Series expansion. [7]

For the analysis of the rocket a commercially available software for students ANSYS was preferred. While doing the fluid analysis around a body we are concerned with the silhouette of the body in the fluid domain. The geometrical model doesn't need to be an exact replica. To study the fluid flow for our case we used the k-epsilon model as it has been tested most widely and has been shown to predict, with the same empirical input, many different flows, including separating and complex three dimensional flows, with an accuracy sufficient for practical purposes. The desired output from the CFD analysis are fins that provide high lifting force with low drag[8].

3. THEORETICAL BACKGROUND

3.1. Rocket Theory

The theory of rockets revolves around Newton's third law of motion, stating that for every action, there's an equal and opposite reaction. Rockets propel themselves by expelling high-speed exhaust gases, generated through controlled combustion of propellants. Key components include the propellant, rocket engine, nozzle, and payload. Flight dynamics involve ensuring stability, controlling trajectory, and understanding orbital mechanics during the flight. A typical flight of a model rocket can be characterized by the four phases[9]:

1. Launch: The model rocket is launched from a vertical launch guide.
2. Powered flight: The motor accelerates the rocket during the powered flight period.
3. Coasting flight: The rocket coasts freely until approximately at its apogee.
4. Recovery: The recovery device opens and the rocket descends slowly to the ground.

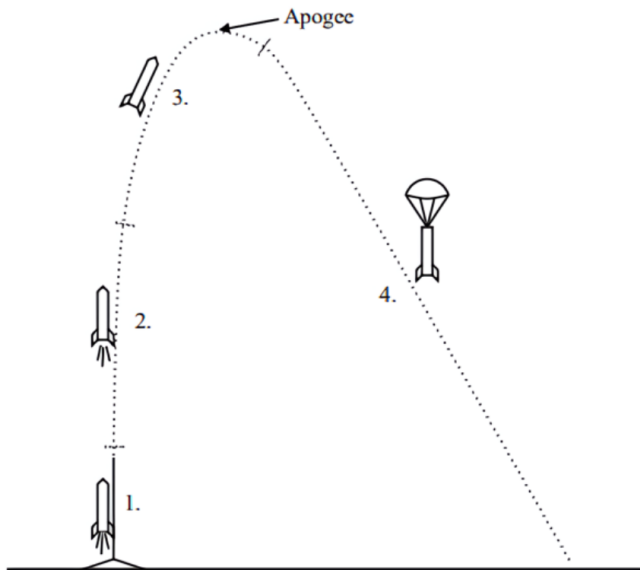


Figure 3.1: Flight Profile

3.1.1. Forces on Rocket

A model rocket encounters three basic forces during its flight: thrust from the motors, gravity, and aerodynamic forces.

Thrust is generated by the motors by exhausting high-velocity gases in the opposite direction. Normally the thrust of a rocket motor is aligned on the center axis of the rocket, so that it produces no angular moment to the rocket.

When the forces and moments generated are summed up, the gravitational force can be seen as a single force originating from the CG. A homogeneous gravitational field does not generate any angular moment on a body relative to the CG.

Aerodynamic forces, on the other hand, produce both net forces and angular moments. To determine the effect of the aerodynamic forces on the rocket, the total force and moment must be calculated relative to some reference point[9].

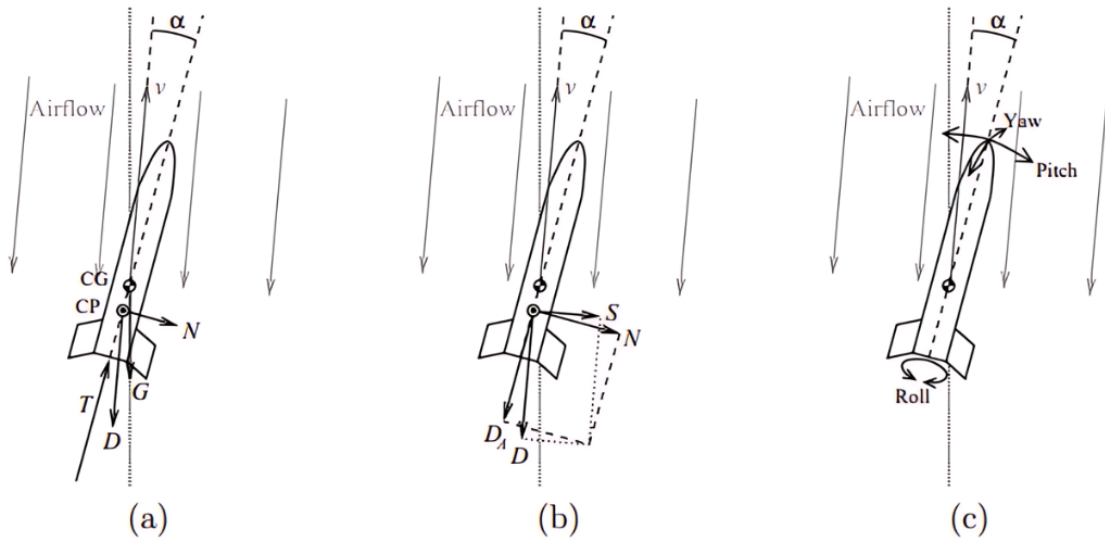


Figure 3.2: Forces acting on Rocket in Free Flight

3.1.2. Stability

Rocket stability refers to the ability of a rocket to maintain orientation and trajectory during flight. Achieving and maintaining stability is crucial for the success of a rocket mission, as unstable flight can lead to unpredictable behavior, loss of control, and potential mission failure.

Static Stability

The static stability of a rocket can be defined as the tendency for a rocket to return to its original position. The behavior of the rocket and how it rotates in response to the wind is best described by the rocket's static stability margin [10].

There are basically three stability conditions for any body, including rockets. They are: positive stability, neutral stability and negative stability. In positive stability, the CG is ahead of the CP; in neutral stability, the CG and CP coincides, whereas in negative stability, the CG is behind the CP. Positive stability is crucial for a rocket to ensure a controlled and successful flight, whereas neutral or negative stability can lead to unpredictable behavior or flight failure. Positioning the CG ahead of the CP and using properly sized and placed fins improves the stability ensuring a steady flight path. A commonly used criterion to quantify rocket stability is the static margin (or stability margin). [11]

$$\text{Static Margin} = \frac{X_{CP} - X_{CG}}{d} \quad (3.1)$$

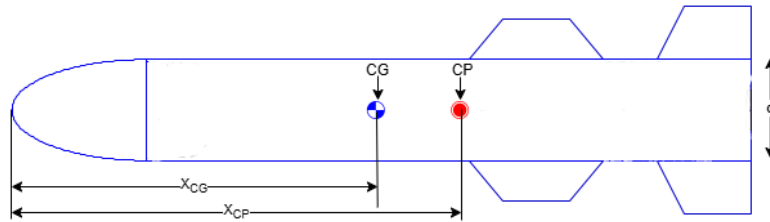


Figure 3.3: Location of CG and CP

Dynamic Stability

A rocket that is statically stable may still be poor at returning the rocket to the original orientation quickly enough. Model rockets may encounter several types of dynamic instability depending on their shape, size and mass.[11]. Dynamic stability refers to the rocket's behavior over time after it has been disturbed. While static stability ensures the rocket has the initial tendency to return to its original position, dynamic stability determines whether it will actually return to that position over time and in what manner. The dynamic response of a system can be used to analyze how a system behaves under a particular dynamic force. For any rocket, determining its dynamic stability is crucial for better understanding of how the rocket behaves after experiencing an external disturbances during flight.

3.1.3. Propellant Theory

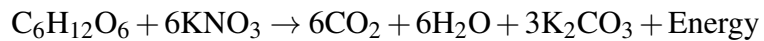
Composition

The composition of the propellant is selected on the basis of availability of the constituents, cost, safety, cast-ability, consistency of performance, and adequate performance. The propellant is composed of Dextrose as fuel and Potassium Nitrate as the oxidizer. The standard ratio of constituents for KNDX is 65 percent Potassium Nitrate and 35 percent Dextrose, by mass. This ratio of oxidizer to fuel mass represents a practical upper limit for "solids" loading of a sugar binder, while maintaining good performance and burn rate characteristics. A higher O/F ratio, and thus higher "solids" loading, may give slightly enhanced performance, but leads to a thicker consistency of the melted mixture (slurry). This makes casting more difficult. The effect of using a lower O/F ratio is reduced performance and a slower burning rate. However, the slurry has a thinner consistency, which makes casting a bit easier. [12].

Combustion

When ignited, the dextrose-based solid propellant undergoes a rapid combustion process that releases large amounts of energy, producing hot gases that expand and create thrust. The combustion reaction involves the oxidation of dextrose by potassium nitrate. As the dextrose burns, it breaks down into carbon dioxide (CO_2) and water vapor (H_2O), while the potassium nitrate decomposes to release oxygen, which sustains the combustion process.

The simplified chemical equation for this reaction is:



This reaction releases significant amounts of thermal energy, which heats the gases produced (mainly CO_2 and H_2O). These gases expand rapidly under the heat, creating high pressure inside the combustion chamber. As the gases are expelled through the rocket nozzle, they generate thrust, propelling the rocket forward according to Newton's Third Law of Motion.

Burn rate

Another important parameter of the propellant is the generalization of properties relating the burn rate at the given chamber pressure which is given by:

$$r = \alpha \cdot P^n \quad (3.2)$$

where α is the pressure coefficient and n is the pressure exponent which determine the overall variation of one property with respect to the change in another. P represents the combustion chamber pressure and r represents the burn rate of the fuel. To determine the values, initially the burn rate of the propellant is determined at different chamber pressure and plotted in a graph. With the curve traced with the data points, the values of α and n can be determined.

Grain Configuration

A cylindrical grain refers to a type of propellant grain where the internal cross-section remains constant along its axis, regardless of the shape of perforations. Perforations are the central cavities or flow passages within a propellant grain, which can have different shapes such as cylindrical, tubular, rod, or star-shaped. The most commonly used grain type is end-burning, where the propellant burns from one end. During motor burn time, neutral burning occurs when the thrust, pressure, and burning surface area remain relatively constant. Progressive burning refers to a burn time where the thrust, pressure, and burning surface area increase, while regressive burning describes a burn time where these parameters decrease. A stoichiometric mixture is one with the correct proportions of fuel and oxidizer for complete combustion, and the balance of oxygen determines whether the propellant is under-oxidized or over-oxidized. At the end of burning, any unburned propellant remaining or expelled through the nozzle is referred to as a sliver[13].

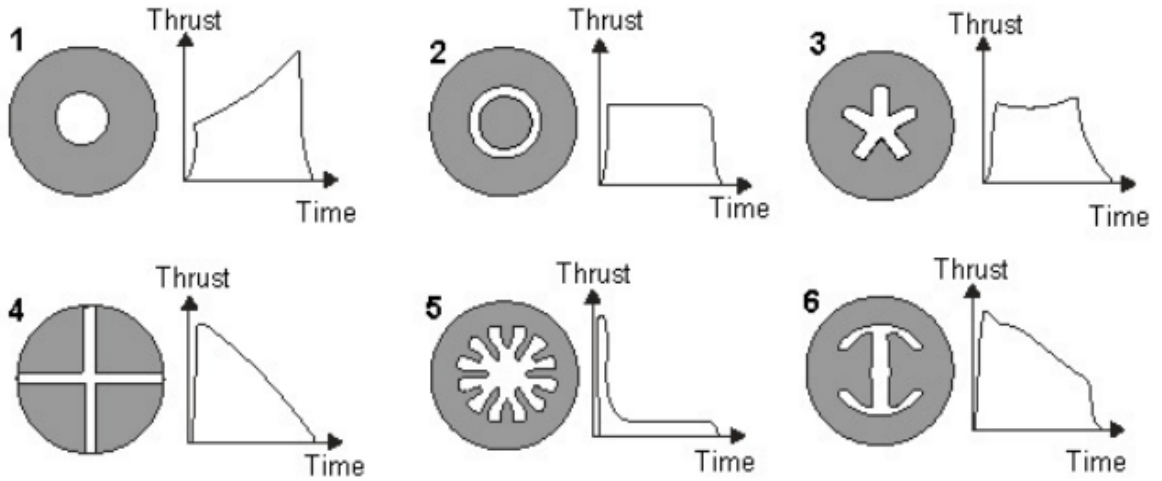


Figure 3.4: Thrust Profile for different grain profiles

3.1.4. Nozzle Theory

Rocket nozzles are crucial components in rocket propulsion systems, designed to accelerate exhaust gases to produce thrust. They efficiently convert the thermal energy of combustion gases into kinetic energy, driving the rocket forward. A well-designed nozzle maximizes the thrust and overall efficiency of the rocket. Rocket engines usually have a fixed geometry CD nozzle with a much larger divergent section.

The amount of thrust produced by the rocket is given as:

$$F = \dot{m} \cdot v_e + A_e \cdot (p_e - p_a) \quad (3.3)$$

The exhaust velocity v_e can be derived from the energy equation for compressible flow in the nozzle, assuming isentropic expansion:

$$v_e = \sqrt{\frac{\gamma - 1}{2\gamma R T_c} \left[1 - \left(\frac{P_c}{P_e} \right)^{\frac{\gamma}{\gamma-1}} \right]} \quad (3.4)$$

The area ratio $\frac{A_e}{A_t}$ (exit area to throat area) is critical for achieving desired exhaust velocities:

$$\frac{A_e}{A_t} = \left(\frac{1}{M_e} \right) \left[\frac{2}{\gamma + 1} \left(1 + \frac{\gamma - 1}{2} M_e^2 \right) \right]^{\frac{\gamma + 1}{2(\gamma - 1)}} \quad (3.5)$$

The throat is the point where the flow transitions from subsonic to sonic, governed by:

$$\frac{A_t}{A^*} = \frac{1}{M} \left(\frac{\gamma+1}{2} \left[1 + \frac{\gamma-1}{2} M^2 \right] \right)^{\frac{\gamma+1}{2(\gamma-1)}} \quad (3.6)$$

where A^* represents the reference area, often equal to the throat area A_t , and M is the Mach number at any point in the nozzle.

Specific impulse measures the efficiency of the rocket engine, representing thrust per unit mass flow rate of propellant:

$$I_{sp} = \frac{V_e}{g_0} \quad (3.7)$$

3.2. Control System

To implement precision stability and especially guidance, static stability is not enough. It needs a control system that controls the vehicle's fins in real time based on the position and orientation of the vehicle. A control system is a set of devices or mechanisms that manages, commands, directs, or regulates the behavior of other devices or systems with a feedback mechanism.

Key Components of a Control System include:

1. Controller: The brain of the control system, it processes inputs and determines the necessary actions to achieve the desired output.
2. Sensors: Devices that measure variables (e.g., temperature, pressure, speed, orientation) and provide feedback to the controller.
3. Actuators: Devices that execute the controller's commands to influence the system (e.g., motors, valves).
4. Set-point: The desired value or state that the control system aims to maintain.
5. Feedback Loop: The process of continuously measuring the output, comparing it to the set-point, and adjusting inputs accordingly.
6. Control Algorithm: Mathematical and logical rules that the controller uses to determine the appropriate control action. There are different control methods like PID control, LQR, MPC adaptive control, or state-space control.

3.3. PID

PID control is one of the most widely used control algorithms in industrial and automation systems due to its simplicity and effectiveness. It combines three types of control actions—proportional, integral, and derivative—to provide a control signal that corrects errors between a desired set-point and the actual process variable.

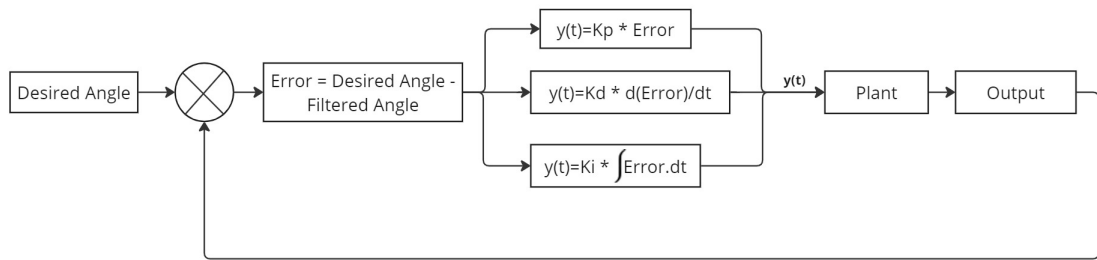


Figure 3.5: PID controller with feedback loop

- **Control Error ($e(t)$):** The difference between the desired set-point $r(t)$ and the measured process variable $y(t)$:

$$e(t) = r(t) - y(t) \quad (3.8)$$

- **Control Output ($u(t)$):** The signal sent to the actuator to correct the error. In PID control, $u(t)$ is computed as the sum of three terms: proportional, integral, and derivative.

1. Proportional Control (P): The proportional term produces an output that is proportional to the current error value. It is the simplest form of control, where the control action is directly proportional to the error.

$$u_P(t) = K_P e(t) \quad (3.9)$$

Where K_P is the proportional gain, which determines the reaction to the current error.

2. Integral Control (I): The integral term is concerned with the accumulation of past errors. If the error has been present for a while, the integral term increases the control output, which helps eliminate residual steady-state errors.

$$u_I(t) = K_I \int_0^t e(\tau) d\tau \quad (3.10)$$

Where K_I is the integral gain, which determines the reaction to the sum of past errors.

- Derivative Control (D): The derivative term predicts future error based on its rate of change. It provides a control output that is proportional to the rate of change of the error, helping to reduce overshoot and improve stability.

$$u_D(t) = K_D \frac{de(t)}{dt} \quad (3.11)$$

Where K_D is the derivative gain, which determines the reaction to the rate of change of the error.

PID Control Equation

The PID control law is the sum of the proportional, integral, and derivative terms:

$$u(t) = K_P e(t) + K_I \int_0^t e(\tau) d\tau + K_D \frac{de(t)}{dt} \quad (3.12)$$

Alternatively, it can be written as:

$$u(t) = K_P \left[e(t) + \frac{1}{T_I} \int_0^t e(\tau) d\tau + T_D \frac{de(t)}{dt} \right] \quad (3.13)$$

where $T_I = \frac{1}{K_I}$ is the integral time and $T_D = K_D$ is the derivative time.

3.4. Kalman Filter

The Kalman Filter is a powerful mathematical tool used in control systems, signal processing, and navigation for estimating the state of a dynamic system from a series of noisy measurements. Named after Rudolf E. Kalman, who developed the filter in the 1960s, it provides optimal estimates by minimizing the mean square error. Its applications range from aerospace and robotics to finance and economics, making it a foundation in modern control theory.

In rocket trajectory estimation, the Kalman Filter can be used to combine measurements from sensors (such as gyroscopes, accelerometers, and GPS) to accurately estimate the rocket's position, velocity, and orientation. The state vector might include position coordinates, velocity components, and attitude angles. The filter recursively updates these estimates based

on sensor data, accounting for noise and disturbances, ensuring accurate tracking of the rocket's trajectory throughout its flight.

KF algorithm differs from the conventional method of timing prediction. It can estimate the system's state via a set of incomplete observations (i.e. missing time points in time-series data) or noisy observations (measurement error). The KF is a fast recursive filter model. It takes up small memory and only needs to retain data for system's state at a time, rather than a long period of time. The actual measured data are used to correct the estimated results[14].

It operates in two main steps: prediction and update. In the prediction step, the algorithm estimates the current state. The Kalman Filter operates in two main steps: prediction and update. In the prediction step, it estimates the current state $\hat{x}_{k|k-1}$ and error covariance $P_{k|k-1}$ based on the previous state estimate, control inputs, and the state transition matrix F_k . This step projects forward the state estimate given the dynamics of the system and any control inputs.

$$\hat{x}_{k|k-1} = F_k \hat{x}_{k-1|k-1} + B_k u_k \quad (3.14)$$

$$P_{k|k-1} = F_k P_{k-1|k-1} F_k^T + Q_k \quad (3.15)$$

where $\hat{x}_{k-1|k-1}$ is the previous state estimate at time $k-1$, B_k is the control input matrix, u_k is the control input at time k , $P_{k-1|k-1}$ is the error covariance matrix of the state estimate at time $k-1$, F_k^T is the transpose of F_k , and Q_k is the process noise covariance matrix.

In the update step, the Kalman Filter incorporates the latest measurement (z_k) to refine the state estimate and its associated uncertainty. The Kalman Gain (K_k) determines how much weight to give to the measurement relative to the predicted state estimate, adjusting the state estimate ($\hat{x}_{k|k}$) and error covariance ($P_{k|k}$) accordingly. [15].

$$K_k = P_{k|k-1} H_k^T (H_k P_{k|k-1} H_k^T + R_k)^{-1} \quad (3.16)$$

$$\hat{x}_{k|k} = \hat{x}_{k|k-1} + K_k (z_k - H_k \hat{x}_{k|k-1}) \quad (3.17)$$

$$P_{k|k} = (I - K_k H_k) P_{k|k-1} \quad (3.18)$$

where H_k is the measurement matrix which maps the state space into the measurement space, H_k^T is the transpose of H_k , R_k is the measurement noise covariance matrix, z_k is the measurement at time k , and I is the identity matrix.

3.5. Computational Fluid Dynamics (CFD)

Computational Fluid Dynamics (CFD) is a tool built on the principle of fluid dynamics that utilizes discretization techniques and solve the problem accordingly in each discrete points. At the beginning of time, to see the behaviour of air flow around body wind tunnels were used but as the time progressed CFD gradually penetrated into the engineering process as a complement to various categories of testing. CFD from being a tool to add depth to information, became a primary source for engineering practice in case of vehicles with narrow flight envelope as missiles or model rockets [16].

The CFD can be used for the conceptual and preliminary design of the rocket. For the final design it is recommended to validate the results with wind tunnel. This strategy of integration is an emerging trend and must be strongly encouraged and developed for the maturation of the CFD approach [17]. The fins of rocket, whether active or passive, plays a massive role in maintaining stability. CFD can be used to explore various configuration of the fins and how they correlate with the interested parameter as the drag & lifting forces.

4. METHODOLOGY

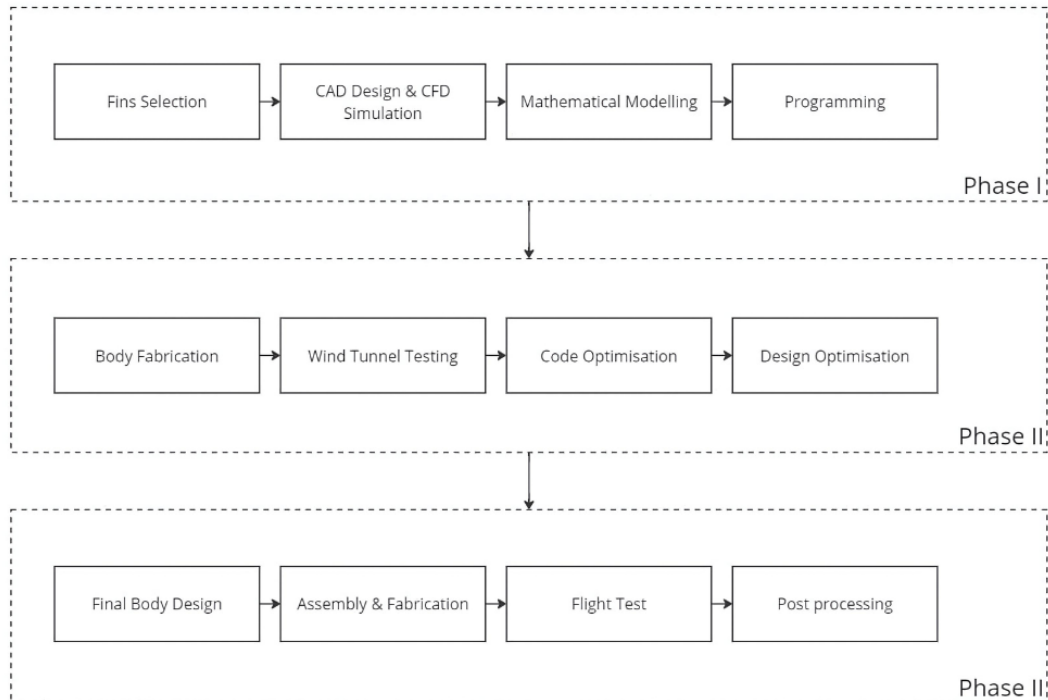


Figure 4.1: Methodology

4.1. Control system

Designing a control system involves several steps:

1. Modeling the System: Creating a mathematical representation of the system's dynamics.
2. Choosing Control Strategy: Selecting between different control methods like PID control, adaptive control, or state-space control.
3. Implementing Controllers: Designing and programming the controllers based on the chosen strategy.
4. Simulation and Testing: Using simulations to predict system behavior and conducting real-world tests to validate the design.
5. Optimization and Tuning: Adjusting parameters to improve performance and efficiency.



Figure 4.2: Control system

4.1.1. Mathematical Modeling

AeroVECTOR, model rocket simulator designed for active control system development and tuning is used for the mathematical modeling of our active fins-controlled rocket to analyze its stability and simulate guidance. This involved defining key flight parameters, modeling fin dynamics, assessing stability, and implementing guidance algorithms to optimize trajectory control. The following methodology outlines the step-by-step process to effectively simulate and tune the rocket's active control system for achieving robust flight stability and accurate guidance:

1. Define Rocket and Flight Parameters: Input essential parameters such as the rocket's mass, center of gravity (CG), moment of inertia, aerodynamic coefficients (lift, drag), and environmental factors like wind and air density, which will influence flight dynamics.
2. Fin Dynamics Modeling: Model the active control fins' dynamics, including actuator behavior and deflection range. Implement a feedback control system, such as a PID controller, to manage fin movements and ensure stability during flight.
3. Stability Analysis: Simulate small disturbances to assess the interaction between the center of pressure (CP) and center of gravity (CG). This analysis ensures that the rocket recovers from instability and maintains controlled flight. Additionally, evaluate the rocket's pitch, yaw, and roll to assess overall stability.
4. Guidance Simulation: Implement guidance algorithms, such as Proportional Navigation or PID controllers, to adjust the fins and steer the rocket along the desired path. Run simulations to fine-tune the control parameters, minimizing trajectory deviations and ensuring precise guidance.
5. Post-Processing and Optimization: Analyze simulation outputs like flight trajectory, fin control efforts, and stability metrics. Use the data to adjust parameters like fin gains and actuator responses, optimizing the system for better stability, accuracy, and control efficiency.

4.1.2. Control system Algorithm

The following block diagram represents the algorithm of our control system.

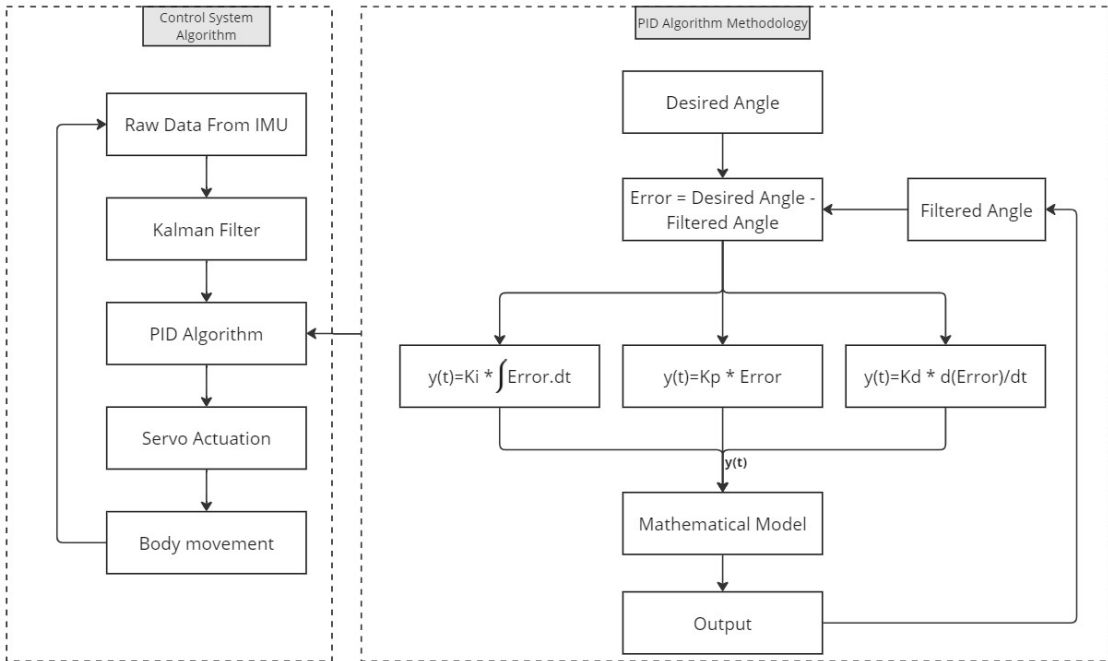


Figure 4.3: Control system Programming Algorithm

This diagram outlines the control system and PID algorithm methodology for a system that uses IMU data to achieve precise angle control. The control system algorithm starts by collecting raw data from the IMU, which is then filtered using a Kalman filter to reduce noise and provide more accurate data. The filtered data are fed into a PID algorithm, which determines the necessary corrections and sends signals to the servo actuators. These actuators adjust the movement of the body to the desired angle.

The methodology of the PID algorithm begins with the definition of a desired angle. The system calculates the error as the difference between the desired angle and the filtered angle from the IMU data. The proportional component of the PID algorithm multiplies this error by a proportional gain. The integral component takes the integral of the error over time and multiplies it by an integral gain. The derivative component takes the derivative of the error over time and multiplies it by a derivative gain. These components are combined to produce the control output $y(t)$. This output is then used to adjust the system, ensuring that it accurately achieves the desired angle. In summary, the system processes IMU data with a Kalman filter, computes adjustments with a PID algorithm, and uses servo actuation to correct body movement, maintaining a specified angle accurately.

4.2. Flight Computer Development

4.2.1. Schematic Representation

The flight test will be conducted for two different rockets that have different flight computers of each as shown in table 4.1. The following block diagram represents the different flight computers developed for different rockets:

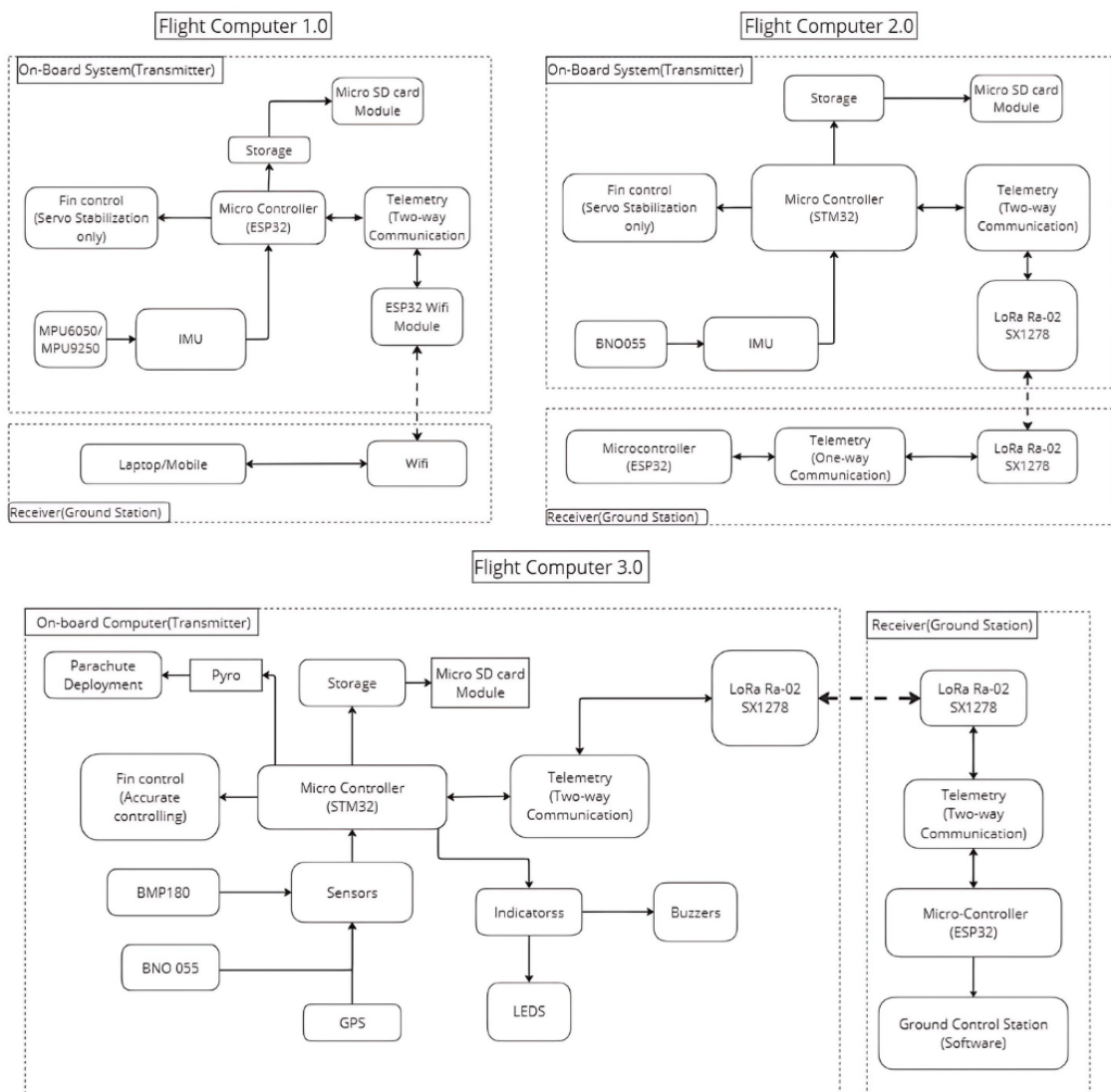


Figure 4.4: Flight Computer Schematic

Flight Computer 1	Flight Computer 2
Esp32	Teensy 4.1
SD card module	Internal Memory
MPU6050	BNO085
SG90 servos	BMS-127WV+
BMP180	BMP180
Buck-Boost	Buck-Boost
Lo-Ra Module	Lo-Ra Module

Table 4.1: Flight Computer 1 V/s Flight Computer 2

4.2.2. Programming Algorithm

The following block diagram represents different flight computer programming algorithms to be developed in different phases of our project:

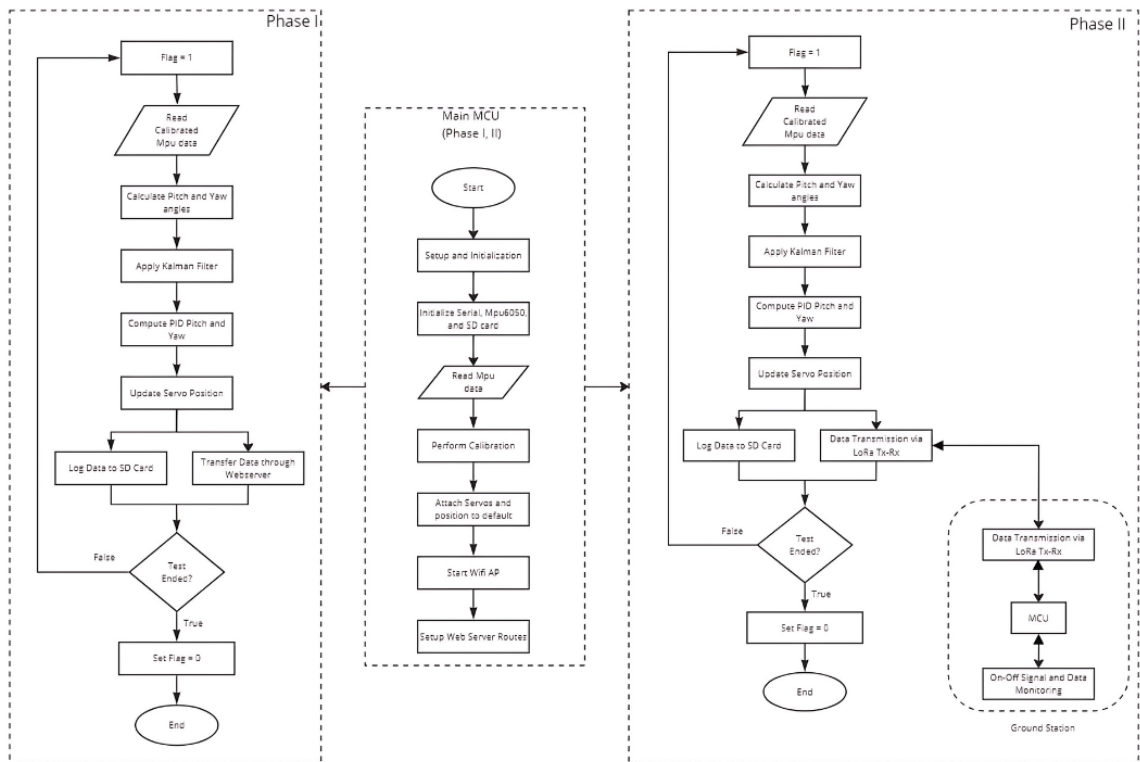


Figure 4.5: Main Programming Algorithm

4.2.3. PCB Designing and Fabrication

PCB is the most crucial part of our project as we will be developing multiple hardware components in our avionics system. Before designing the PCB, the circuit was checked

and verified using breadboard and matrix board. After verification, the PCB designing was started. For schematic and PCB editing, KiCad software was used and the traces were given suitable width based on their functionality. For fabrication, the PCB design was printed in a glossy paper using printing ink. The ink was then transferred on a cleaned copper board using acetone. After this etching process was carried out. The etching is done by putting the copper board on the solution of HCl and Hydrogen Peroxide in the ratio of 1:3. In 5 minutes, the PCB was ready. Our PCB was fully operational after the drilling and soldering tasks.

The PCB is a crucial part of our project, as it integrates multiple hardware components in our avionics system. Before designing the PCB, we checked and verified the circuit using breadboards and matrix boards. Once verified, we proceeded to PCB designing using KiCad software for schematic and PCB editing. The traces were assigned suitable widths based on their functionality.

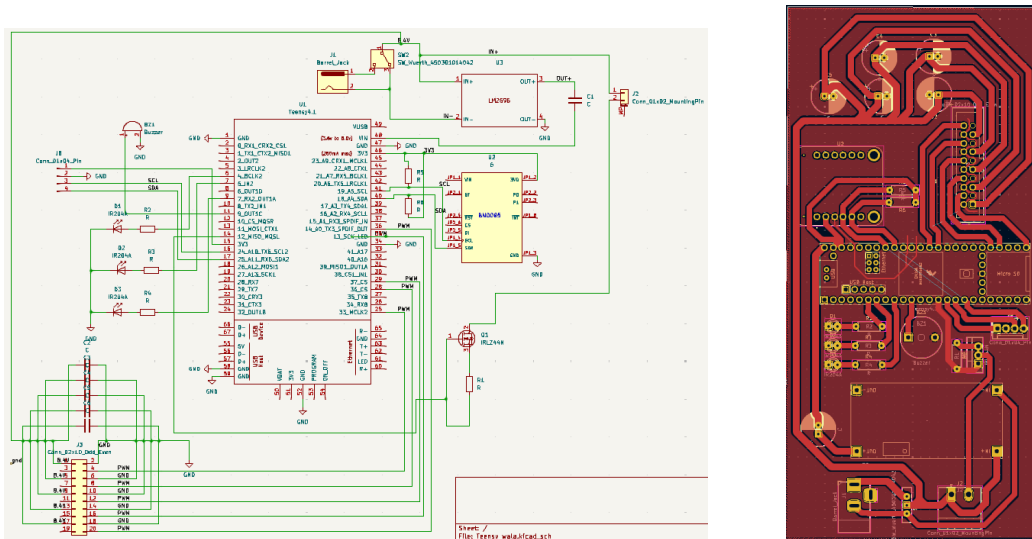


Figure 4.6: PCB Schematic and PCB Design

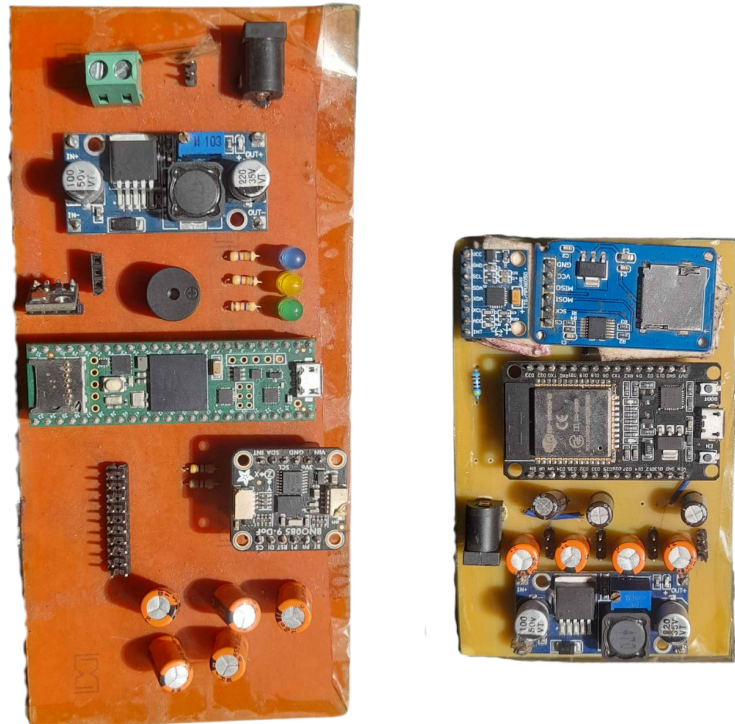


Figure 4.7: Avionics Bay

4.3. Vehicle Development

4.3.1. Body Fabrication

The fuselage has been made using glass fiber composite in the composite lab. The fins, mechanical linkages, and nose cone have all been 3D printed using PLA+ material because of its complexity to meet the design requirements.

450 GSM Fiberglass composites was chosen for the fabrication of rocket body. The mold for the body fabrication was 75mm PVC pipe. A layer of printing paper and a outer layer of cello tape was winded around the pipe for the easiness of mold release after the composite gets settled.



Figure 4.8: Design and Fabrication of Phase I

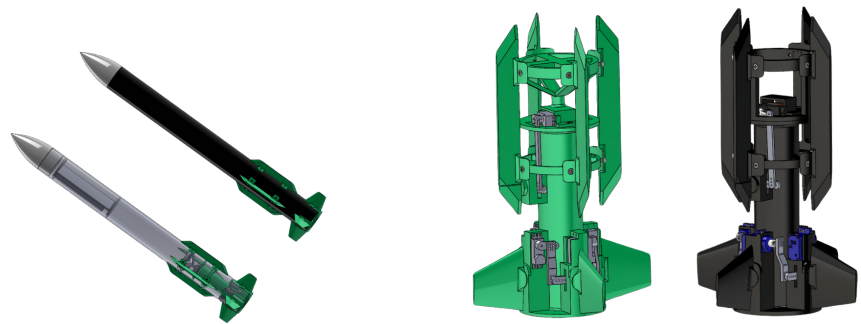


Figure 4.9: CAD Design of Phase II

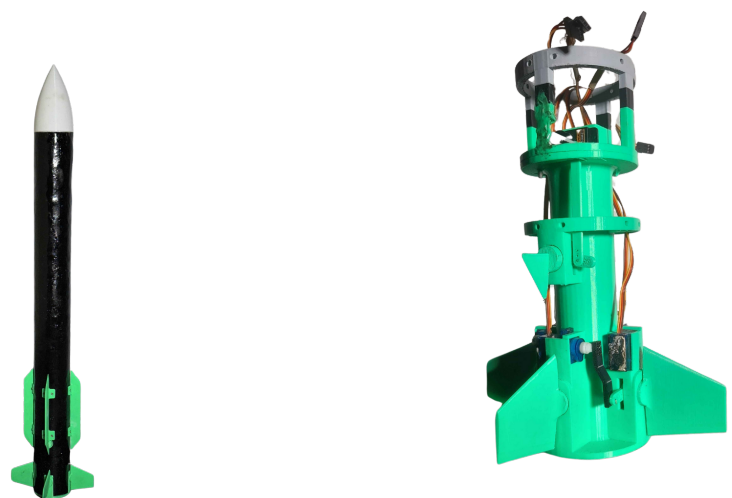


Figure 4.10: Fabrication of Phase II

4.3.2. Propulsion System

Propellant Preparation

Potassium nitrate KNO_3 is used as the oxidizer, and Dextrose is used as the fuel. Dextrose is chosen to increase the burn time, allowing for longer flight durations and enabling more flight data to be gathered and extended maneuvers to be performed. Dextrose is commercially available as Glucose-D. This form of dextrose is known as dextrose monohydrate, which is 91 percent dextrose by weight, with the remainder present as molecular bound water. As such, the ratio of potassium nitrate to dextrose monohydrate must be adjusted to achieve a given oxidizer/fuel (O/F) ratio. In other words, the required amount of dextrose monohydrate required in the mixture must be multiplied by 1.1, which is the ratio of Molecular Weights (198.18/180.16) [12]. The fuel is prepared by heating a solution of KNO_3 and dextrose using an induction heater until the crystallization point is reached. An oxidizer-to-fuel ratio of 65:35 is used.



Figure 4.11: Propellant Grain of KNDX Propellant

Static Thrust Measurement

The static thrust is measured in a Thrust Stand. Loadcell is the sensor used to measure thrust in Newton. The signal from loadcell is amplified using an amplifier HX711 and the data is processed through a Arduino Nano microcontroller. Using this thrust curve, we can analyse and obtain the required fuel composition to achieve desired burn time.



Figure 4.12: Setup for Static Thrust Measurement

Ignition System

The rocket ignition system uses nichrome wire and gunpowder to initiate the motor. A container of gunpowder is positioned above the motor and facing its grain structure. When an electric current passes through the nichrome wire, it heats up, igniting the gunpowder. This ignition triggers a pressure increase within the container, causing the diaphragm to release. This ignition technique ensures simultaneous contact between the ignited gunpowder and the entire length of the fuel grain, promoting a lateral burn and effectively increasing the booster's burn rate. As a result, the rocket experiences enhanced thrust performance during flight.

Motor Casing

The motor dimensions are determined by using simulation software like Openmotor to obtain the desired output. The casing is made from light weight and heat resistant material using glass fiber. The rocket motor is also made up of 450 GSM Fiberglass composite. The mold for the motor was a 32mm pipe. A layer of printing paper and an outer layer of cello tape were wound around the pipe for the easiness of mold release after the composites get set.



Figure 4.13: Composite Rocket Motor

Nozzle

The nozzle needs to be lightweight too. For that, we have used graphite nozzle. The graphite nozzle may have some problem of irrosion, to encounter this silicone grease, which is a flame resistant lubricant is used. The nozzle design is done using Openmotor, Meteror and Ansys simulation and is manufactured using lathe.



Figure 4.14: Fabrication of Nozzle using Lathe



Figure 4.15: Graphite Nozzle

4.3.3. Nose Cone and Fins

The nose cone and fins of the body was fabricated using 3D printer. The 3D printing technique was chosen due the complexity of structure and difficulties in manufacturing.

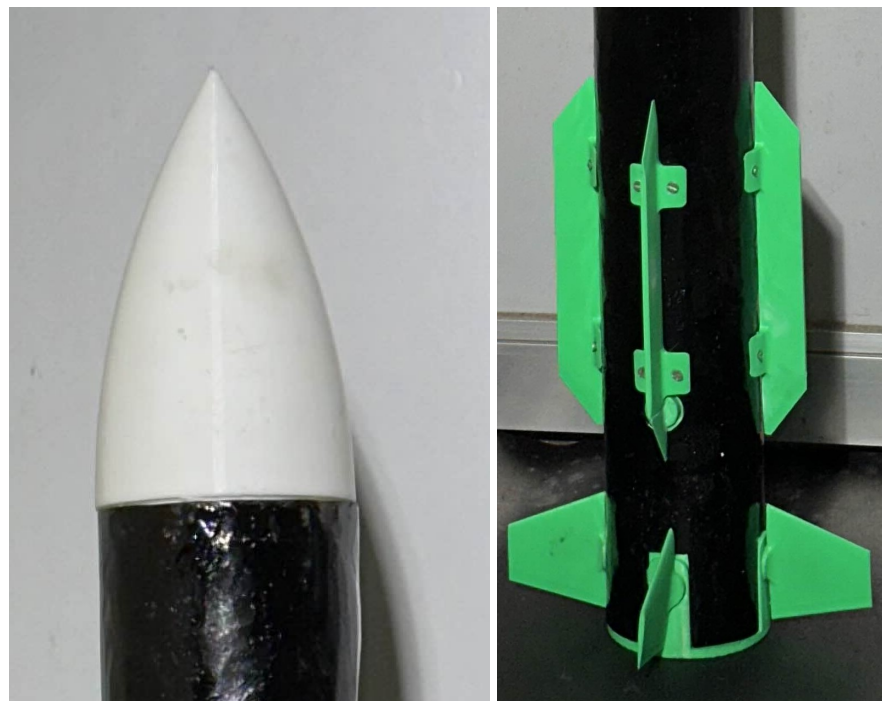


Figure 4.16: Motor For Black Powder Propellant

Figure 4.17: Fragments of Motor After Test

4.3.4. Recovery System

The recovery system consists of a parachute, shock cord and canister. Black powder is filled inside the canister. We are using pyro ejection technique for the recovery of the

rocket. It uses an ejection charge, in our case it is the black powder to deploy parachute that slows the rocket's descent and allows for a safe landing.

4.3.5. Servo Housing and Linkages

Two different servo housing was designed for different test body. SG90 servos is used in one housing and BMS-147WV+ is used in another. The design of the servo housing was influenced by the size of rocket motor and the body tube as it should fit right in between the rocket motor. The housing and linkages was 3D printed using PLA+. The servo housing and linkage mechanism for the fins is as shown in Fig . A total of five servos is used in the rocket body, four for the pitch and yaw moment and one for the roll moment. The servo is placed around the rocket motor. The servos is attached to the fins through the linkage mechanism. This housing is attached to the body frame by using bearings.



Figure 4.18: Servo Housing and Linkages

4.4. Stability Analysis

The rocket's stability needs to be ensured before commencing any other phases of the project. We are making a fin controlled rocket which mainly handles the dynamic stability while obviously contributing to the static stability along with canard. The stability analysis shows the control effectiveness of the fins in achieving the stability.

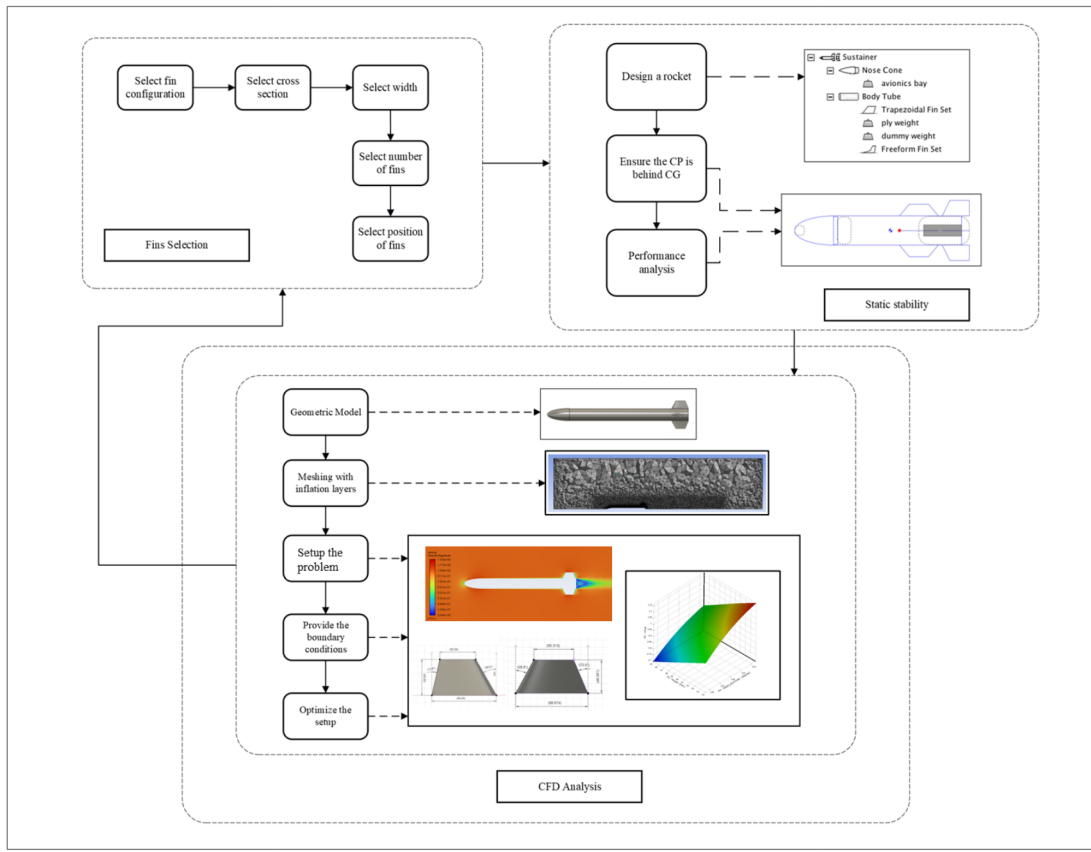


Figure 4.19: Stability Analysis

4.4.1. Selection of fins

The geometrical parameters that defines the fins are its cross section, tip chord ratio, cant angle, sweep angle, effective aspect ratio and width. Initially, a baseline four-fins configuration with geometric parameters from historical data and a low fidelity tool XFLR5 was selected. The maximum velocity of the rocket will be about Mach 0.3 and the Reynold number is in the range of 5.6e06. The NACA 0015 airfoil was selected with the structural integrity and Cl vs alpha graph. Even though NACA 0012 has a steeper curve the width was taken as a margin for the structural integrity and NACA 0015 was selected. Regarding the shape as well the trapezoidal performed the best.

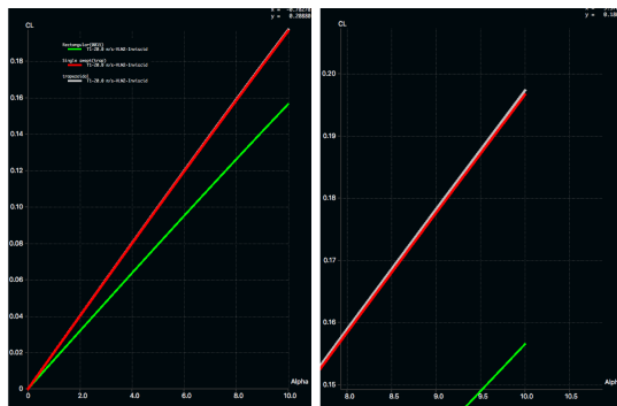


Figure 4.20: Airfoil Selection and Closeup

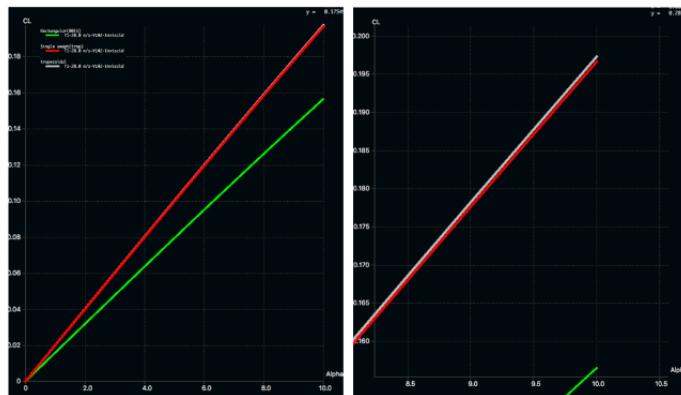


Figure 4.21: Shape Selection and Closeup

4.4.2. Static Stability Analysis

The static stability of the rocket is calculated using OpenRocket. The software is used to design the rocket ,determine the stability margin and its performance. The rocket design is optimized within the software till it is made statically stable with suitable margin. A good rule of thumb is of 1-2 calibers. This also includes the shift of the cp at extreme angle of attack.

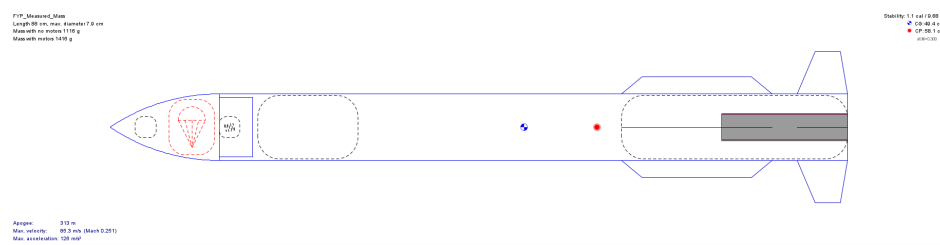


Figure 4.22: Rocket Design in OpenRocket

4.4.3. CFD Analysis

For the CFD analysis, Ansys 2022 is used. A high fidelity tool is necessary to get accurate data for a rocket launch hence a steady state simulation is done to measure the drag and lift forces from the fin. The Direct Optimization tool in Ansys is used for the optimization of fins.

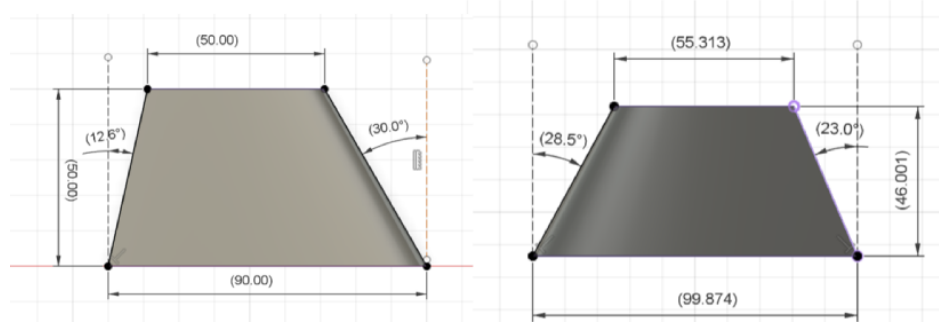


Figure 4.23: Baseline vs Optimized Fin

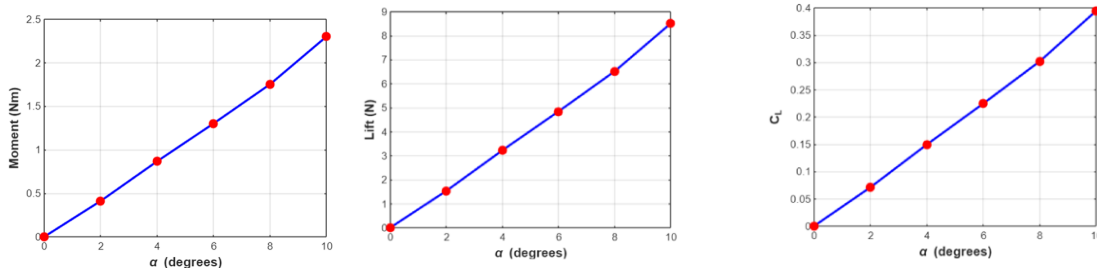


Figure 4.24: Properties of Optimized Fins

4.5. Wind Tunnel Testing

The wind tunnel is used to tune the PID controller and to validate the data from simulations. A setup is made that allows the movement of the model in only one axis. Two rectangular frames of plywood assembles the setup. The outer frame is attached to a frame which is stationed ahead of the wind tunnel and is connected to the inner frame through a shaft-bearing attachment. The inner frame is used to clamp the test body. The bearings are used to allow the moment of test body in only one axis. Both the pitch and yaw moment can be tested using this setup. For the test of roll moment, the nose of the body is suspended from the front of a table fan so that the roll moment can be induced. The data thus obtained from the test is further processed using MATLAB to analyze the behaviour of the model.

The speed of the wind was around 5 m/s at full power and as our objective of the test was to check the control authority, the test at even at this speed was reasonable. The test was performed by giving deflection of different angles. The response of the body after the deflection was measured using MPU6050. The measured data was the pitch angle of the body.

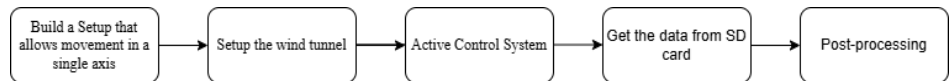


Figure 4.25: Wind Tunnel Flowchart



Figure 4.26: Setup for Wind Tunnel Test

4.6. Servo Selection

Different types of servos are used in each of the flight test body: SG90 and BMS-127WV+. SG90 servo was selected due to its availability and the characterization of this servo was done to validate its capability to control the fins in flight conditions. For BMS-127WV+, the amount of torque required for the rotation of fins in flight condition was calculated and based on the result this servo was selected. Its operating speed is 0.05 sec/60° at the operating power of 8.4V.

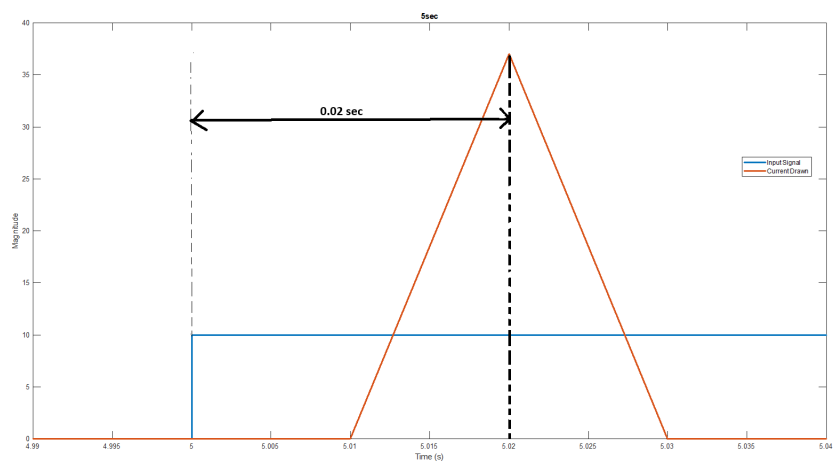


Figure 4.27: Lag Response Test of SG90

5. RESULTS AND DISCUSSIONS

5.1. Output

5.1.1. Static Thrust Test

The static thrust test of KNDX propellant was accomplished twice. The three-grain motor was used where the length of each grain was 50mm, with grain diameter of 30 mm and core diameter of 10mm. Both the test showed similar result with the simulation.

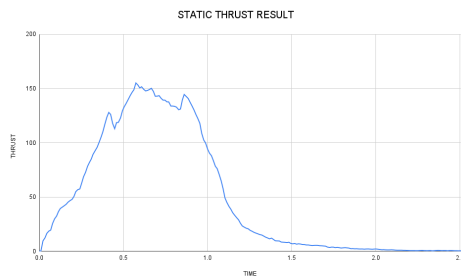


Figure 5.1: Static Thrust Test I

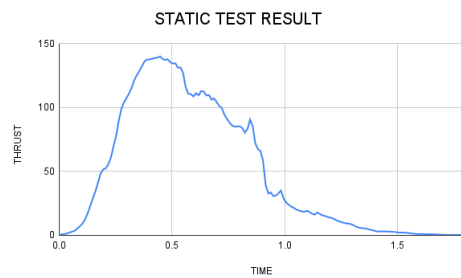


Figure 5.2: Static Thrust Test II

5.1.2. Wind Tunnel Test

The wind tunnel test was performed to verify the control authority of the control system. In one experiment, a ten degree set-point was given and the body held a stable position at around eight degree.

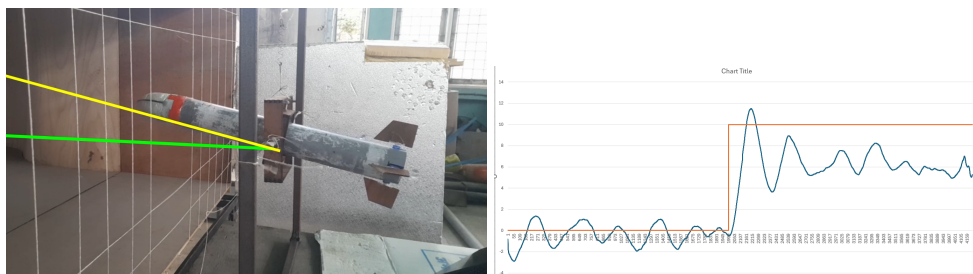


Figure 5.3: Wind Tunnel Test

5.1.3. Recovery Test

For Recovery of our rocket, the ejection test was performed to verify the recovery algorithm and parachute ejection system. In one experiment, a pulley was used to pull the rocket upward first, to simulate the launch, and then the pulley was lowered to simulate descent. The rocket was programmed to eject after 3 metre descent from the apogee. The test was successful



Figure 5.4: Wind Tunnel Test

5.2. Work Completed

The project has made a significant progress with the targeted amount of tasks ahead of mid-term is almost complete. The completed tasks include the design and assembly of flight computer I, II and III , the mathematical modeling of the rocket body with active fins, the CFD analysis for the optimization of the control fins, the design and

fabrication of graphite nozzle, the rocket motor design and fabrication, propellant selection, the linkage and servo housing design and fabrication, basic PID tuning, body fabrication for the wind tunnel test and flight test.

5.2.1. Propellant test

A total of three other different propellant formulation was tested:

KNSU Propellant

The propellant is composed of Sucrose as fuel and Potassium Nitrate as the oxidizer. The standard ratio of constituents for KNSU is as shown in table [5.1]. This formulation of propellant had low burn time then required. Higher burn time for higher flight time is required for the flight test. Hence, KNSU propellant was discarded as a propellant for flight test.

Formulation	Potassium Nitrate (%)	Sucrose(%)
KNSU	64.0	35.0

Table 5.1: Formulation Table for KNSU Propellant

Black powder propellant

Black powder, commonly known as gun powder was prepared with a proportion as shown in table[5.2]. Potassium nitrate and Sulfur was brought from the market and Charcol was prepared by heating wood above 400° C (750° F) in an oxygen-starved environment. When wood is burnt in a limited supply of oxygen until water and other volatile substances are removed, the remaining residue is called as charcoal. Then the gun powder was prepared by ball milling of mixture for around 10-12 hrs.

Gunpowder propellant was tested using end burning. The chamber pressure was so high during the test that the rocket motor got burst. Hence, this formulation was not suitable for the flight test.

Formulation	Potassium Nitrate (%)	Charcol (%)	Sulphur (%)
Black Powder	75.0	15.0	10.0

Table 5.2: Formulation Table for Black Powder Propellant



Figure 5.5: Motor For
Black Powder Propellant



Figure 5.6: Fragments of
Motor After Test

Epoxy based Composite Propellant

Composite propellants was also tested to increase burn time. The formulation of the composite propellant is shown in the table [5.3] (all are mass percentages) [12]:

Formulation	Resin : hardener	Potassium Nitrate (%)	Epoxy (%)	Ferric Oxide (%)
RNX-57	6:1	70.0	22.0	8.0

Table 5.3: Formulation Table for RNX-57 Propellant Mixture

But due to high flame temperature, it melted the glass fiber motor casing and no significant thrust was measured.



Figure 5.7: Burnt Motor After Test

5.2.2. Nozzle Fabrication

A total of four other different nozzle than the graphite nozzle was used during the testing phase of the propellant and motor. Initially, PVC Rocket motor was used to test the gun powder propellant by end burning. In this test, the nozzle was made using PVC bush with the convergent and divergent section made up of mseal. Later after the selection of KNDX as our propellant for flight test nozzle of sheet metal, mud and composites was tested.



Figure 5.8: Mold for Composite Nozzle



Figure 5.9: Composite Nozzle



Figure 5.10: Bush Nozzle with Mseal as Convergent and Divergent Section



Figure 5.11: Sheet Metal Nozzle

All of these different nozzle was tested because of their light weight and easy to manufacture features. But, the nozzle of sheet metal didn't choke the flow and didn't give result of required amount of thrust. The nozzle of mud and composites had problem

of erosion and was not suitable enough for the flight test.

The graphite nozzle was then tested and the result was suitable enough for the flight hence it is chosen for the flight test.

5.2.3. Catapult Test

To check control system of the rocket, an un-powered flight test using catapult was tested. The rubber elastic used in the catapult was unable to provide enough impulse for enough flight time to check the control system and get proper data. The flight time of the un-powered flight was only about one second. The focus of the team then shifted from un-powered flight test to powered flight test.



Figure 5.12: Catapult Test

5.3. Work Remaining

The Flight Test Phase I which was scheduled before the mid-term will happen in the following week of the mid-term defense. Other remaining works include the improvement of the propellant composition to increase flight time, further tuning of PID controller and works regarding the guidance of the rocket.

5.4. Limitations

- Required sensors and servos not available in Nepal and some even in India so had to source them from USA.
- Limitation in the speed of the available windtunnel.
- Budget management for buying the required materials.
- Difficulty to perform launch test frequently due to permission and budget restrictions.

5.5. Problems Faced

- Our project faces regulatory limitation from CAAN due to the apogee at which we will be reaching.
- We encountered issues with the material to be used for the nozzle due to the light weight constraints before getting hand on graphite. The static thrust test was also delayed because of this.
- We faced difficulties with the proper formulation of propellant for required burn time.

5.6. Budget Analysis

S.N	Name of Particulars	Cost (NRs.)
1	Micro Controller	30,000
2	Sensors	10,000
3	PCB Fabrication	5,000
4	Power Management system	5,000
5	Communication	5,000
6	Body Fabrication	20,000
7	Propulsion	10,000
8	Recovery	5,000
9	Travel Expenses	30,000
10	Miscellaneous	10,000
Total		1,30,000

Table 5.4: Budget Analysis

5.7. Gantt chart



Figure 5.13: Timeline

6. CONCLUSION AND FUTURE ENHANCEMENT

6.1. Conclusion

The static thrust test and the wind tunnel test showed promising result to proceed into the flight test. The result of recovery test also showed promising result for recovery after hitting the apogee. The final body tube fabrication for the flight is completed and the flight test will take place in the next week after the mid-term. The fabrication of the nose cone, electronics bay and propulsion system have also been completed. In the flight test, initially command of only roll control will be given to the control system. After the control of roll moment within five degrees, pitch moment command will be given to the control system. The commands for the second flight test will depend on the result of the first flight test.

6.2. Scope For Future enhancement

The fuel composition for the motor needs to be made so as to generate required thrust for desired amount of time to be able to perform all control moves. This would also enhance the quality of data collected which will further help to enhance the control algorithm and mathematical model.

References

- [1] “Roll reversal phenomenon control in flight vehicles,” *Aerospace Science and Technology*, vol. 79, pp. 413–425, 2018.
- [2] A. Datye, G. Bandodkar, S. Syeda, and S. Manchkanti, “Effects of shark caved fins on altitude performance of a high-powered rocket,” *2019 NCUR*, 2019.
- [3] A. Datye, “Fin optimization for enhanced flight performance of an experimental rocket,” in *Proceedings of The National Conference On Undergraduate Research*, 2018, pp. 5–7.
- [4] G. di Pasquo, “Aerovector,” Universidad Tecnológica Nacional – Regional Haedo, Tech. Rep., 2020.
- [5] R. Sumathi and M. Usha, “Pitch and yaw attitude control of a rocket engine using hybrid fuzzy-pid controller,” *The Open Automation and Control Systems Journal*, vol. 6, no. 1, 2014.
- [6] A. B. Kisabo, A. F. Adebimpe, O. C. Okwo, and S. O. Samuel, “State-space modeling of a rocket for optimal control system design,” in *Ballistics*. IntechOpen, 2019.
- [7] C. Montella, “The kalman filter and related algorithms: A literature review,” *Res. Gate*, pp. 1–17, 2011.
- [8] W. Rodi, “Examples of turbulence models for incompressible flows,” *AIAA journal*, vol. 20, no. 7, pp. 872–879, 1982.
- [9] S. Niskanen, “Openrocket technical documentation,” *Development of an Open Source model rocket simulation software*, pp. 11–13, 2013.
- [10] V. A. Guerrero, A. Barranco, and D. Conde, “Active control stabilization of high power rocket,” 2018.
- [11] G. H. Stine and B. Stine, “Handbook of model rocketry,” Wiley, 2004.
- [12] R. A. Nakka, “Solid propellant rocket motor design and testing,” Ph.D. dissertation, University of Manitoba, 1984.
- [13] A. F. El-Sayed, *Fundamentals of aircraft and rocket propulsion*. Springer, 2016.
- [14] D. Simon, *Optimal State Estimation: Kalman, H Infinity, and Nonlinear Approaches*. Wiley, 2006. [Online]. Available: https://books.google.com.np/books?id=UiMVoP_7TZkC
- [15] R. E. Kalman, “A new approach to linear filtering and prediction problems,” 1960.

- [16] M. R. Malik and D. M. Bushnell, “Role of computational fluid dynamics and wind tunnels in aeronautics r and d,” Tech. Rep., 2012.
- [17] D. Favier, “The role of wind tunnel experiments in cfd validation,” *Encyclopedia of Aerospace Engineering*, 2010.